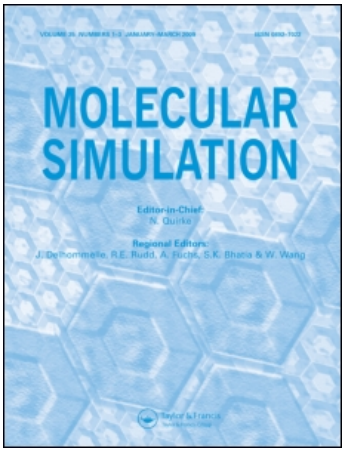

Molecular Simulation
Publication details, including instructions for authors and subscription information:
http://www.informaworld.com/smpp/title~content=t713644482

Computer Modelling Studies of Elastic and Ion Transport Properties of Yttria Stabilised Cubic Zirconia

P. J. Chaba[a]; P. E. Ngoepe[bc]
[a] Department of Physics, University of the North, Sovenga, South Africa [b] Materials Modelling Centre, University of the North, Sovenga, South Africa [c] MATTER Division, CSIR, Pretoria, South Africa

To cite this Article Chaba, P. J. and Ngoepe, P. E.(1998) 'Computer Modelling Studies of Elastic and Ion Transport Properties of Yttria Stabilised Cubic Zirconia', Molecular Simulation, 21: 2, 161 — 171
To link to this Article: DOI: 10.1080/08927029808022057
URL: http://dx.doi.org/10.1080/08927029808022057

Molecular Simulation, 1998, Vol. 21, pp. 161–171
Reprints available directly from the publisher
Photocopying permitted by license only

COMPUTER MODELLING STUDIES OF ELASTIC AND ION TRANSPORT PROPERTIES OF YTTRIA STABILISED CUBIC ZIRCONIA

P. J. CHABA [a] and P. E. NGOEPE[b,c,*]

[a] *Department of Physics, University of the North, Sovenga 0727, South Africa;*
[b] *Materials Modelling Centre, University of the North, Sovenga 0727, South Africa;*
[c] *MATTEK Division, CSIR, PO Box 395, Pretoria 0001, South Africa*

(Received January 1998; accepted January 1998)

A comparison of calculated and experimental temperature variation of the elastic constants was used to predict types of oxygen-vacancy dopant clusters in yttria stabilised cubic zirconia, which serves as an electrolyte in solid oxide fuelcells. Such clusters were incorporated in supercells set up for molecular dynamics studies, where oxygen transport properties were investigated at concentrations of 9.4 and 24 mol% of yttrium oxide and up to 1600 K.

Keywords: Computer modelling; elastic constants; oxygen diffusion; $ZrO_2(xY_2O_3)$

INTRODUCTION

Solid oxide fuel-cells that use yttrium-stabilized cubic zirconia, $ZrO_2(x-Y_2O_3)$, as electrolyte are being studied extensively owing to their outstanding ionic conductivity and mechanical properties [1]. Pure zirconium oxide is monoclinic at room temperature, however, it can be stabilised in a cubic fluorite structure by doping with a minimum of 8 mol% Y_2O_3. Oxygen vacancies are created for charge compensation as the concentration of yttrium is increased. EXAFS [2] and previous computer modelling [3] studies have shown that vacancies are preferably located at next-nearest neighbour sites to yttrium.

Measurements of temperature variation of elastic constants of cubic $ZrO_2(xY_2O_3)$ have shown two regions of interest [4]. Firstly a linear decrease

* Corresponding author.

of elastic constants was noted from ambient to a transition temperature (T_c) to a high temperature phase. This behaviour was accounted for by lattice anharmonicity using quasi-harmonic approach [5]. Secondly a pronounced deviation from linearity occured above T_c, and was ascribed to an onset of a fast-ion phase associated with development of disorder on the oxygen sublattice, by analogy with previous studies of flourites [6]. An increase in the dopant concentration led to reduction in $\partial C_{ij}/\partial T$ above T_c; an effect that was related to defect–defect repulsive contributions to the free energy. Furthermore, the value of T_c tends to decrease with increasing yttrium concentration and has values of 1300 and 1050 K for 9.4 and 24 mol% Y_2O_3 respectively.

In a recent molecular dynamics study of $ZrO_2(xY_2O_3)$ [7] it was reported that diffusion occurs predominantly on the oxygen sublattice. A maximum in oxygen diffusion was noted near 8 mol% Y_2O_3. The study further revealed that an increase in $Y^{3+}-Y^{3+}$ neighbour clusters tend to trap more oxygen vacancies than isolated Y^{3+}. More such neighbour clusters tend to occur at higher concentrations of Y_2O_3 and lead to reduced oxygen diffusion. However, the orientation of the yttria oxygen-vacancy clusters was chosen randomly in these studies.

A comparison of experimental and calculated elastic constants has assisted in clarifying types of defects in LaF_3 [8]. In the current study temperature variation of elastic constants, calculated from energy minimisation methods, will be compared with Brillouin scattering results [6] in order to predict the configuration of dopant vacancy complexes that occur in $ZrO_2(xY_2O_3)$. Such clusters will be incorporated in supercells used for molecular dynamics studies where diffusion coefficients and ion migration mechanisms are determined at different yttrium concentrations and temperatures.

COMPUTATIONAL PROCEDURE

Distorted fluorite structured $ZrO_2(xY_2O_3)$ supercells containing approximately 96 ions were set up, where $x = 9.4$ and 24 mol%. The supercells included yttrium oxygen-vacancy clusters, with orientations shown in Figure 1.

The energy minimisation procedure was applied on resulting structures at constant volume, to determine equilibrium configurations. Associated thermodynamic quantities were calculated. In all cases, the computer

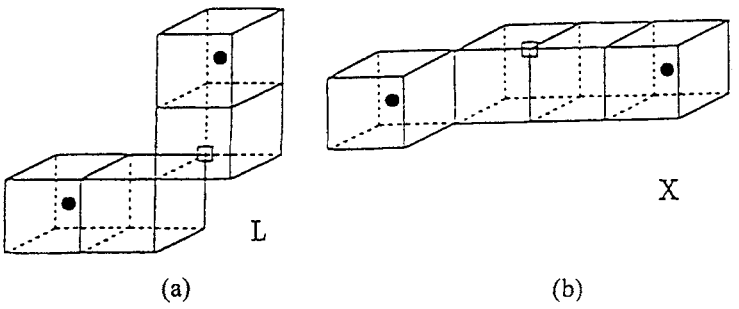

FIGURE 1 Different orientations of oxygen-vacancy yttrium clusters, namely L and X shaped.

code THBREL [9] was used. Temperature changes of elastic constants were determined by lattice expansion, within the quasi-harmonic approximation. Interionic potentials employed in our calculations are given in Table I.

Molecular dynamics technique involves solution of Newton's second law of motion. Using suitable algorithms, trajectories and velocities of ions are determined. Diffusion coefficients, D_i, may be obtained from Einstein like relationship

$$\langle r_i^2 \rangle = 6D_i t + B$$

where $\langle r_i^2 \rangle$ is the mean square displacement and B is a constant. FUNGUS [10] program was used in the present study and details of the calculation are given in Table II:

TABLE I Shell model interionic potentials for $ZrO_2(xY_2O_3)$

Interaction shell model	*Shell charges*		*Spring constant k*
Zr(core)–Zr(Shell)	1.350		169.617
Y(core)–Y(shell)	−0.25		145.00
O(core)–O(shell)	−2.07719		27.29
Short range potentials	*A(eV)*	*ρ(A)*	*C(eVA^{-6})*
$Zr_4^+ - O^{2-}$	985.87	0.376	0
$Y^{3+} - O^{2-}$	1345.10	0.349	0
$O^{2-} - O^{2-}$	22764.30	0.149	27.89

TABLE II Details of molecular dynamics calculations

Simulation box	8 unit cells of $ZrO_2(xY_2O_3)$
Timestep	5 fs
Startup	Initial structure: distorted fluorite
	1000 steps for equilibration
	7000 steps (35 ps) for a run
Temperatures	300–1600 K
Rigid ion potentials were used	

RESULTS AND DISCUSSIONS

Energy Minimisation Calculations

As mentioned in the introduction, the aim of this section is to identify possible types of yttria oxygen-vacancy complexes that are dominant in yttria stabilised zirconia. In accordance with previous EXAFS and computer simulation studies clusters were chosen such that oxygen vacancies were located at nearest neighbour sites to yttria ions. Furthermore, clusters were classified according to how yttria ions were oriented relative to oxygen vacancies; examples are L and X shaped clusters shown in Figure 1.

We now compare linear changes of the calculated and measured elastic constants (C_{ij}) with increasing temperature; where computations involved different types of clusters. Figures 2a and b show calculated temperature variations of elastic constants (C_{11}, C_{12} and C_{44}) associated with the L-shaped clusters. In Figure 2a all elastic constants, related to 9.4 mol% concentration, change linearly with temperature up to 1300 K. Elastic constants for the 24 mol% Y_2O_3 vary similarly up to 1000 K (Fig. 2b); in agreement with experimental observations below T_c [4]. An onset of pronounced deviation of elastic constants from linearity above T_c, particularly in 24 mol% Y_2O_3, is also consistent with results from experiments. It is, however, noted that although the calculations predict changes above T_c, they fail to reproduce a correct $\partial C_{ij}/\partial T$ in the fast-ion phase, owing to inadequacy of the quasi-harmonic approximation in yielding magnitudes associated with the fast-ion phase.

It is interesting to note how other cluster types, for example the *X* shaped cluster, have a different influence on changes of elastic constants. In Figures 3a, associated with 9.4 mol% Y_2O_3 and Figure 3b, related to 24 mol% Y_2O_3, linearity of $\partial C_{ij}/\partial T$ ends near 800 K, which is significantly lower than corresponding experimental T_cs. Such behaviour was prevalent in most clusters that are different from the *L*-shaped cluster. Hence it may be

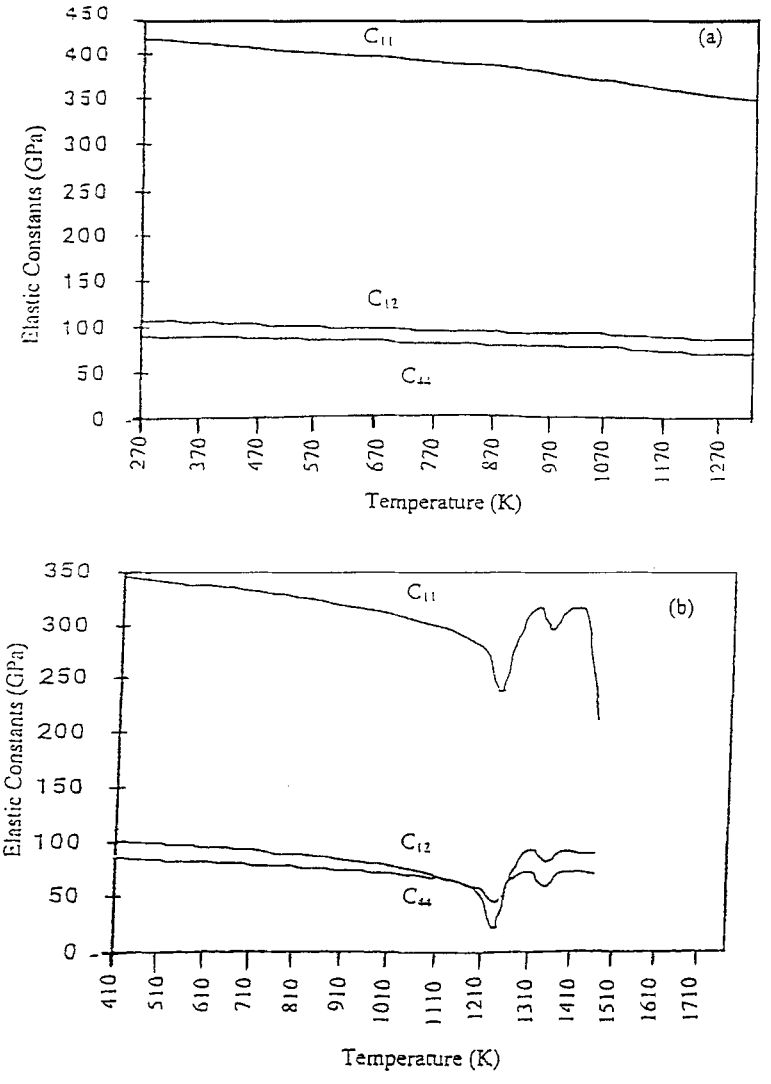

FIGURE 2 Calculated temperature variation of elastic constants of $ZrO_2(xY_2O_3)$ for the L-shaped clusters in; (a) $x = 9.4$ mol % (b) $x = 24$ mol%.

surmised that the L shaped cluster reproduces the experimental linear behaviour of elastic constants more reliably.

Table III compares magnitudes of calculated and experimental slopes of $\partial C_{ij}/\partial T$ related to various cluster models, below T_c. In Table IIIa, it is remarkable how the L shaped model yields slopes that are in agreement with

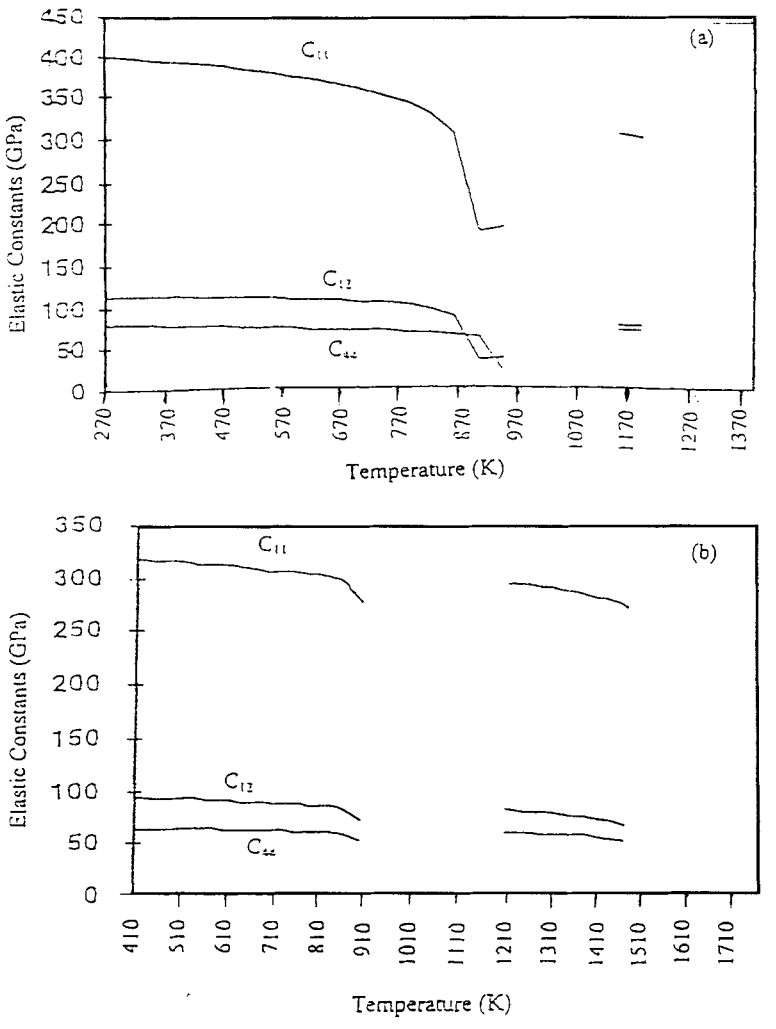

FIGURE 3 Calculated temperature variation of elastic constants of $ZrO_2(xY_2O_3)$ for the X-shaped cluster; (a) $x = 9.4$ mol% (b) $x = 24$ mol%.

experiments, for the three elastic constants at a concentration of 9.4 mol%. The model further reproduces increased slopes of all elastic constants at 24 mol% Y_2O_3 (Tab. IIIb) very well. It is noted that results emanating from other clusters deviate significantly from experimental values, at two concentrations mentioned above, the extreme case being where vacancies and dopants are randomly distributed in supercells. Such comparison of calculated and experimental elastic constants was previously used to suggest

TABLE III Calculated and experimental slopes of temperature variation of elastic constants of $ZrO_2(xY_2O_3)$, at different values of x

a)	$ZrO_2(9.4\,mol\%\ Y_2O_3)$		
Configuration	$\partial C_{11}/\partial T$	$\partial C_{12}/\partial T$ (GPa/K)	$\partial C_{44}/\partial TX$
X	0.030	0.010	0.015
L	0.051	0.021	0.015
XL	0.036	0.015	0.012
Random	0.125	0.010	0.033
Experimental	0.050	0.020	0.012
b)	$ZrO_2(24\,mol\%\ Y_2O_3)$		
Cluster	$\partial C_{11}/\partial T$	$\partial C_{12}/\partial T$ (GPa/K)	$\partial C_{44}/\partial T$
X	0.037	0.025	0.013
L	0.055	0.032	0.024
Random	0.036	0.015	0.019
Experimental	0.055	0.036	0.020

anion Frenkel disorder as the dominant high temperature disorder in LaF_3 [8]. Hence it could be used to show preference for the L shaped cluster in $ZrO_2(xY_2O_3)$.

Molecular Dynamics Calculations

In previous molecular dynamics studies dopant charge compensating vacancy complexes in yttria stabilised zirconia were chosen more randomly. Our energy minimisation calculations have shown preference for the L-shaped vacancy dopant clusters, hence these complexes will be used for the current molecular dynamics studies, from 300 to 1600 K. In agreement with previous molecular dynamic studies [7], no diffusion was noted on the cation sub-alttices. Consequently attention will be focussed on the oxygen sublattice.

The change of mean square displacements of oxygen ions with time for $ZrO_2(9.4\,mol\%\ Y_2O_3)$, at several temperatures, is shown in Figure 4a.

TABLE IV Anion diffusion coefficients in $ZrO_2(xY_2O_3)$

Temperature (K)	*Calculations* $9.4\,mol\%$	*Diffusion coefficient* $10^{-6}\,cm^2/s$ $24\,mol\%$	*Experimental* $10.2\,mol\%$
2073			1.9 [16]
1600	0.742	0.49	
1000	0.235	0.068	
300	0.0	0.0	

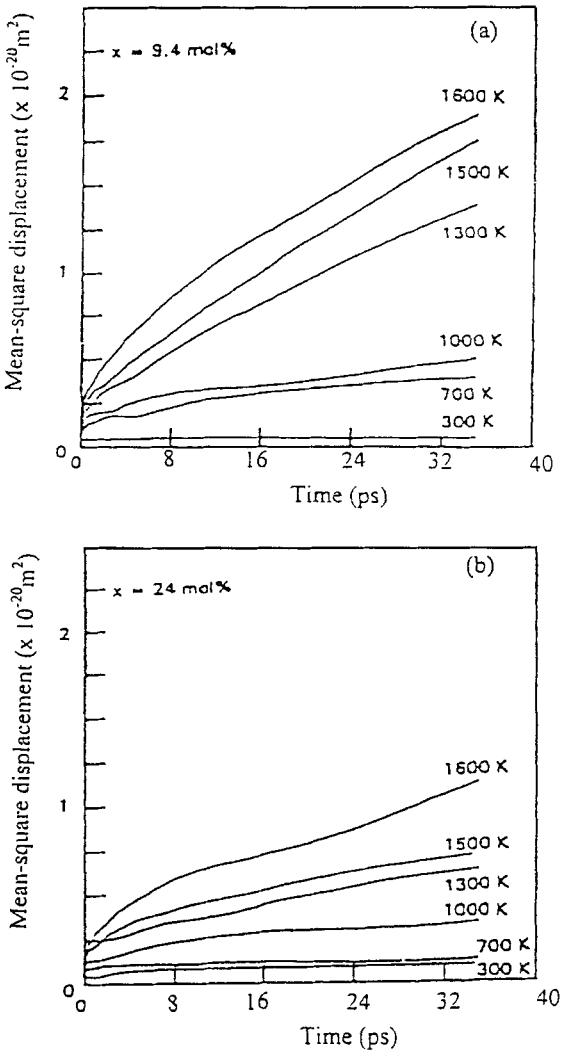

FIGURE 4 Change of mean square displacement with time of $ZrO_2(xY_2O_3)$ at different temperatures for; (a) $x = 9.4$ mol% (b) $x = 24$ mol%.

Diffusion is almost absent at 300 K and it increases progressively from 700 K up to the highest calculated temperature, 1600 K. Oxygen diffusion in the ZrO_2(24 mol% Y_2O_3) is notable at higher temperatures (Fig. 4b). A striking feature in $ZrO_2(xY_2O_3)$ is enhanced oxygen ion motion below T_cs, at both concentrations. In contrast diffusion tends to occur above T_c in pure fluorine ion conductors with the fluorite structure [11, 12]. However, the

presence of substantial diffusion below T_c has been mentioned in molecular dynamics studies of CaF_2(10 mol% LaF_3) [11] and Raman scattering investigation of LaF_3(5 mol% BaF_2) [13], which are all doped fluorine ion conductors. Hence some of the mechanisms responsible for fluorine diffusion below T_c in doped fluorine ion conductors could account for high oxygen mobility at lower temperature in $ZrO_2(xY_2O_3)$.

The presence of considerable dopant concentrations affects oxygen diffusion. It is apparent from Figure 5, that oxygen diffusion for 24 mol% Y_2O_3 is more limited than for 9.4 mol% Y_2O_3. In fluorine ion conductors, molecular dynamics studies have shown that fluorine diffusion is quite rapid in pure CaF_2 and reduces on doping [11]. The retarded ionic motion was attributed to defect repulsive interactions. In the recent molecular dynamics study on $ZrO_2(xY_2O_3)$ reduced ion motion at higher concentration was ascribed to an increasing number of $Y^{3+} - Y^{3+}$ neighbour pairs which tend to trap oxygen vacancies.

One of the important features of molecular dynamics studies has been the determination of atomistic mechanisms controlling bulk transport properties. Figure 5 shows the nature of ion migration mechanisms from trajectory plots for a period of 35 ps. In Figures 5a and b oxygen ion trajectories of 9.4 mol% Y_2O_3 and 24 mol% Y_2O_3 concentrations are shown respectively at a temperature of 300 K. It is obvious that ions vibrate around one lattice

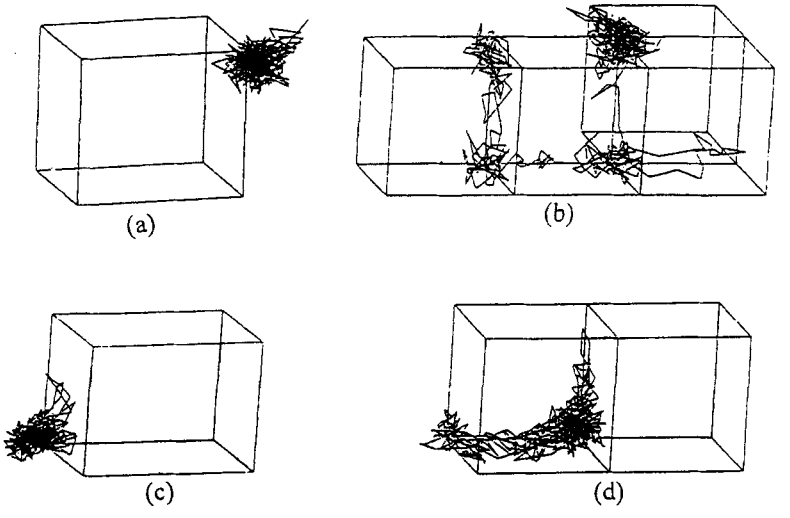

FIGURE 5 Oxygen ion trajectories of $ZrO_2(xY_2O_3)$ for a period of 35 ps.; (a) x = 9.4 mol%, T = 300 K, (b) x = 9.4 mol%, T = 1600 K, (c) x = 24 mol%, T = 300 K, (d) x = 24 mol%, T = 1600 K.

site for the entire period of the simulation. Figures 5c and d depict migrations of oxygen ions at 9.4 and 24 mol% Y_2O_3 respectively at 1600 K. Oxygen ions reside at a lattice site for a considerable time and hop to the next one along the ⟨100⟩ direction. Hence it may be concluded that whereas oxygen diffusion is negligible at room temperature, it proceeds predominantly by a hopping vacancy mechanism at higher temperatures. This type of motion is consistent with lower calculated oxygen vacancy as compared to interstitial activation energy, for both 9.4 and 24 mol% Y_2O_3 concentrations [14]. The prevalence of anion vacancy motion was reported in pure alkaline-earth fluorides [11]. On the contrary interstitialcy motion appears to be dominant in rare-earth doped alkaline-earth fluorides [11] and mixed metal fluorides [15]. Differences in migration mechanisms between our current $ZrO_2(xY_2O_3)$ and doped rare-earth fluorides may suggest that the nature of disorder responsible for the fast-ion phase in these systems is different.

CONCLUSION

The accuracy with which the L shaped model reproduces the experimental linear behaviour and temperature slopes of elastic constants in $ZrO_2(xY_2O_3)$ below T_c, at the two investigated concentrations, puts it forward as the most likely defect configuration to occur. Molecular dynamics study has shown that oxygen diffusion occurs below T_c, and reduces with increasing dopant concentration. Lastly the oxygen vacancy motion appears to be prevalent. Studies involving a wider range Y_2O_3 concentrations will be valuable.

Acknowledgements

The authors would like to thank C. R. A. Catlow and J. D. Comins for useful discussions.

References

[1] Matze, Hj (1991). "Ion transport in ceramics", *Phil. Mag.*, **64**, 1181.
[2] Catlow, C. R. A., Chadwick, A. V., Greaves, G. N. and Moroney, L. M. (1986). "EXAFS study of yttria stabilised zirconia", *J. Am. Cer. Soc.*, **69**, 272.
[3] Dwivedi, A. and Cormack, A. N. (1989). "Stability of Phases $CaZrO_3$ and $CaZr_4O_9$ incorporated in the system $CaO-ZrO_2$", *J. Solid State Chem.*, **79**, 218.
[4] Botha, P. J., Chiang, J., Comins, J. D., Mjwara, P. M. and Ngoepe, P. E. (1993). "Behavior of elastic constants, refractive index, and lattice parameter of cubic zirconia at high temperatures", *J. Appl. Phys.*, **73**, 7287.

[5] Comins, J. D., Ngoepe, P. E. and Catlow, C. R. A. (1990). "Brillouin scattering and computer simulations studies of fast ion conductors: a review", *J. Chem. Soc. Faraday Trans.*, **86**, 1183.
[6] Catlow, C. R. A., Comins, J. D., Germano, F. A., Harley, R. J. and Hayes, W. (1978). "Brillouin scattering and theoretical studies of high-temperature disorder in fluorites crystals", *J. Phys. C*, **11**, 3197.
[7] Li, X. and Hafskjold, B. (1995). "Molecular dynamics studies of yttrium stabilized zirconia", *J. Phys. Condens. Matter*, **7**, 1255.
[8] Ngoepe, P. E., Jordan, W. M., Catlow, C. R. A. and Comins, J. D. (1990). "Computer modeling and Brillouin scattering studies of anharmonicity and high-temperature disorder in LaF_3", *Phys. Rev. B*, **41**, 3815.
[9] Catlow, C. R. A. and Mackrodt, W. C. (1982). In: "Computer Simulation of Solids", Catlow, C. R. A. and Mackrodt, W. C., Eds., Lecture Notes in Physics, Vol. 166, Springer, Berlin, Ch. 1.
[10] Walker, J. R. (1982). In: "Computer Simulations of Solids", Catlow, C. R. A. and Mackrodt, W. C., Eds. Lecture Notes in Physics, Vol. 166, Springer, Berlin, Ch. 5.
[11] Ngoepe, P. E. and Catlow, C. R. A. (1991). "Molecular dynamics study of ion transport in CaF_2 (10 mol% LaF_3)", *Radiation Effects and Defects in Solids*, **119**, 399.
[12] Netshisaulu, T. T., Ngoepe, P. E., Comins, J. D. and Catlow, C. R. A. (1992). "Ion transport studies in CdF_2", *Proceedings of the XII International Conference on Defects in Insulating Materials*, Karnet, O and Spaeth, J.-M., Eds., World Scientific Publishers, p. 979.
[13] Anghel, C. A. I. and Comins, J. D. (1997). "Brillouin and Raman scattering measurements on superionic LaF_3 and LaF_3 (BaF_2)", **239–241**, 413.
[14] Chaba, P. J. (1998). *M. Sc. Dissertation*, University of the North.
[15] Netshisaulu, T. T. (1996). *M. Sc. Dissertation*, University of the North.
[16] Suemoto, T. (1990). "Quasi-elastic light scattering in superionic conductors", *Solid State Ionics*, **40/41**, 250.